DOI: 10.6060/tcct.20165912.5514

Для цитирования:
Шефер Л., Ищенко А.А., Жабанов Ю.А., Отлётов А.А., Гиричев Г.В. Динамика фотодиссоциации неупорядоченных молекулярных ансамблей по данным метода дифракции электронов с временным разрешением. *Изв. вузов. Химия и хим. технология*. 2016. Т. 59. Вып. 12. С. 22–31.

For citation:
Schafer L., Ischenko A.A., Zhabanov Yu.A., Otlyotov A.A., Girichev G.V. Photodissociation dynamics of randomly oriented molecular ensembles by time-resolved electron diffraction. *Izv. Vyssh. Uchebn. Zaved. Khim. Khim. Tekhnol.* 2016. V. 59. N 12. P. 22–31.

УДК: 544.13

Л. Шефер, А.А. Ищенко, Ю.А. Жабанов, А.А. Отлётов, Г.В. Гиричев

Лотар Шефер

Кафедра Химии и Биохимии, Университет штат Арканзас, Фейетвилл, США
E-mail: schafer@uark.edu

Анатолий Александрович Ищенко (✉)

Кафедра аналитической химии Института тонких химических технологий Московского технологического университета, проспект Вернадского, 86, Москва, Российская Федерация, 119571
E-mail: aischenko@yasenevo.ru (✉)

Юрий Александрович Жабанов, Арсений Андреевич Отлётов, Георгий Васильевич Гиричев

Кафедра физики Ивановского государственного химико-технологического университета, Шереметевский пр., 7, Иваново, Российская Федерация, 153000
E-mail: zhabanov@gmail.ru, otlyotov@isuct.ru, girichev@isuct.ru

ДИНАМИКА ФОТОДИССОЦИАЦИИ НЕУПОРЯДОЧЕННЫХ МОЛЕКУЛЯРНЫХ АНСАМБЛЕЙ ПО ДАННЫМ МЕТОДА ДИФРАКЦИИ ЭЛЕКТРОНОВ С ВРЕМЕННЫМ РАЗРЕШЕНИЕМ

Введение времени в дифракционные методы и разработка основополагающих принципов их анализа открывает новую методологию для изучения переходных состояний центров реакции и короткоживущих промежуточных соединений в газообразных и конденсированных средах. В данной статье мы предлагаем основные элементы теории, которые могут быть использованы при анализе данных, полученных методом TRED для хаотически ориентированных лазеро-возбужденных молекул. Разработанная теория применима к процессам фотодиссоциации свободных молекул. Теория иллюстрируется моделированием фотогенерированной диссоциации молекул ICN. На основе модельных расчетов, представленных в этой статье, мы приходим к выводу, что методом TRED возможно исследование когерентной динамики процессов фотодиссоциации. Зависящие от времени данные метода TRED позволяют наблюдать динамику фотодиссоциации при реалистичном значении временного разрешения метода, составляющего 300 фс, что достигается в ряде экспериментальных установок метода TRED.

Ключевые слова: дифракция электронов с временным разрешением, переходные состояния реакционных центров, процессы фотодиссоциации, когерентная динамика фотодиссоциации

UDC: 544.13

L. Schafer, A.A. Ischenko, Yu.A. Zhabanov, A.A. Otlyotov, G.V. Girichev

Lothar Schafer

Department of Chemistry and Biochemistry, University of Arkansas, Fayetteville, AR, USA
E-mail: schafer@uark.edu

Anatoly A. Ischenko (✉)

Department of Analytical Chemistry, Moscow University of Technology, Institute of Fine Chemical Technologies, Moscow, 119571, Russia
E-mail: aischenko@yasenevo.ru (✉)

Yury A. Zhabanov, Arseniy A. Otlyotov, Georgiy V. Girichev

Department of Physics, Ivanovo State University of Chemistry and Technology, Sheremetievskiy ave., 7, Ivanovo, 153000, Russia
E-mail: zhabanov@gmail.ru, otlyotov@isuct.ru, girichev@isuct.ru

PHOTODISSOCIATION DYNAMICS OF RANDOMLY ORIENTED MOLECULAR ENSEMBLES BY TIME-RESOLVED ELECTRON DIFFRACTION

The introduction of time in diffraction methods and the development of foundational principles of their analysis opens up new methodologies to study transient states of the reaction centers, and short-lived intermediate compounds in gaseous and condensed media. In the current article, we propose the basic elements of the theory that can be employed in analyses of TRED data recorded from randomly oriented laser-excited molecules. The formalism is applicable to photodissociative processes and to nuclear dynamics studies of photodissociation phenomena. The theory was illustrated by modeling the diffraction intensities of photogenerated dissociation of ICN molecules. Based on model calculations presented in this article we conclude that, by TRED method, time-dependent coherent dissociation dynamics can in principle be resolved at a realistic time scale that significantly shorter than the electron pulse duration of 300 fs, which is achieved at present in a number of TRED experiments.

Key words: time-resolved electron diffraction, transient states of the reaction centers, photodissociative processes, coherent dissociation dynamics

INTRODUCTION

In the beginning of 1980's, the diffraction paradigm was formulated: implementing electron diffraction with time resolution adds a temporal coordinate to the determination of molecular structures [1-4]. Time-resolved electron diffraction (TRED) rested on the concept of flash photolysis originally proposed by Norrish and Porter in 1949 [5]. Advances in the generation of X-ray pulses have made possible the closely related time-resolved X-ray diffraction (TRXD) [6]. In both methods, short laser pulses create the transient structures and induce chemical dynamics that are subsequently imaged by diffraction at specific points in time.

TRED and TRXD as methods for structural and dynamic studies of fundamental properties differ from traditional diffraction methods in both the experimental implementation and in the theoretical approaches used to interpret the diffraction data [7, 8]. The transition to the picosecond and femtosecond temporal scales raises numerous important issues related to the accuracy of the dynamic parameters of the systems studied by analyzing time-dependent scattering intensities. There is a particularly pronounced need of corresponding theoretical basis for the processing of the diffraction data and the results of spectral investigations of the coherent dynamics of molecules in the field of intense ultrashort laser radiation. Such a unified and integrated approach can be formu-

lated using the adiabatic potential energy surfaces (APES) of the ground and excited states of the molecular systems under study [9-11].

To understand the dynamic features of molecular systems within the complex landscapes of APES it is necessary to explore them in the associated 4D space-time continuum. The introduction of time in diffraction methods and the development of foundational principles of their analysis opens up new methodologies to study transient states of the reaction centers, and short-lived intermediate compounds in gaseous and condensed media.

The use of pico- or femtosecond bunches of electrons as probes, synchronized with the pulses of the exciting ultrashort laser radiation, and led to the development of ultrafast electron crystallography and nanocrystallographic techniques [12], of dynamic transmission electron microscopy [13-17] and of molecular quantum state tomography [18]. One of the promising applications, developed by the electron diffraction methods, is their use for the characterization and the "visualization" of processes, occurring in the photo-excitation of free molecules and biological objects for the analysis of different surfaces, thin films, and nanostructures (see the recent review articles [19-29]. The combination of state-of-the-art optical techniques and diffraction methods, using different physical principles but complementing each other, opens up new possibilities for structural research at ultrashort time sequences. It provides the required integration of the triad "Structure-Dynamics-Function" in chemistry, biology, and materials science [15, 16, 23].

In the current article, we propose the basic elements of the theory that can be employed in analyses of TRED data recorded from randomly oriented laser-excited molecules. The formalism is applicable to dissociative processes and to nuclear dynamics studies of dissociation phenomena. The theory will be illustrated by modeling the diffraction intensities of photogenerated dissociation of ICN molecules. The results will be compared with our previous modeling studies of randomly oriented molecular ensembles.

1. Theory: basic assumptions and approximations

A plane wave electron that is *elastically* scattered by an atom emerges as a spherical wave with an amplitude given by [30]:

$$\Psi(R,\theta) = \{\exp(ikR)/R\}f(\theta), \quad (1)$$

where R is the distance between the scattering center and the detector plane and the absolute value of the wave vector k is given by $k = |\mathbf{k}| = 2\pi/\lambda$ with λ the wavelength of the electron. For an isolated atom, the atomic electron scattering amplitude $f(\theta)$ determines the amplitude of the electron beam scattered into the angle θ (Fig. 1).

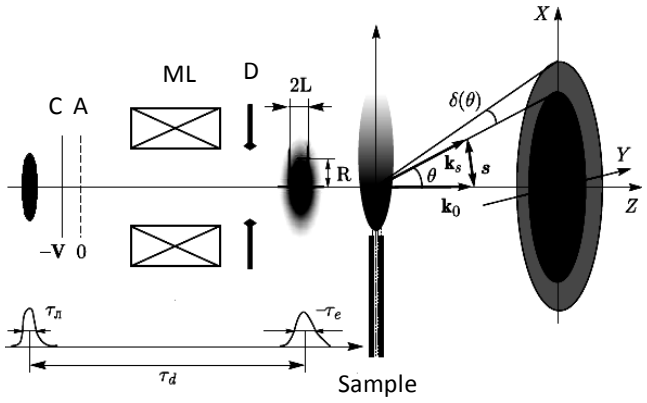

Fig. 1. Scheme of the TRED for random oriented molecules and determination of the coordinates of the scattered electron. θ - the scattering angle, δ (θ) – a correction to the scattering angle caused by Coulomb repulsion in the electron bunch; k_o and k_s - wave vectors of the incident and scattered electrons, respectively; s - momentum transfer vector in the laboratory frame XYZ. C- cathode, A - anode, ML - Magnetic Lenses, D - Diaphragm; τ_L - the duration of the laser pulse, τ_e - electron pulse duration; l - axis of the electron bunch in the direction of its motion, R - axis of the electron bunch in the transverse direction; τ_d - the time delay between the excitation laser pulse and diagnosing electronic pulse
Рис. 1. Схема TRED эксперимента для произвольно ориентированных молекул и определение координат рассеяния электронов. θ – угол рассеяния, δ(θ) – поправка к углу рассеяния, вызванная кулоновским отталкиванием в элект-ронном пучке; k_0 и k_s – волновые векторы падающего и рас-сеянного электронов, соответственно; s – вектор передачи импульса в лабораторной системе координат XYZ; К – катод, А – анод, МЛ – магнитные линзы, Д – диафрагма, τ_L – длительность лазерного импульса, τ_e – длительность электронного импульса, l – ось электронного импульса в направлении его движения, R – ось электронного сгустка в поперечном направлении, τd – время задержки между возбуждающим лазерным импульсом и диагностирующим электронным импульсом

As the electron traverses the atom, it experiences a phase delay, making the scattering factor complex. While for scattering from a single atom this phase shift is inconsequential, scattering from multiple atoms may entail different phase shifts from each individual atom.

The amplitude of the wave scattered by atom i within a molecule is written as [30]:

$$\Psi_i(R,\theta) = \{\exp(i|\mathbf{R}-\mathbf{r}_i|)/|\mathbf{R}-\mathbf{r}_i|\}\exp(ik_0z_i)f_i(\theta), \quad (2)$$

where z_i is the projection of the atomic position vector $\mathbf{r}_i$ onto the Z-axis (Fig. 1) and R is the scattering distance. Since R is a macroscopic parameter (i.e., $r_i << R$), eqn. (2) can be expressed as:

$$\Psi_i(R,\theta) = \{\exp(ikR)/R\}\exp[i(\mathbf{k}_0-\mathbf{k}_s)\mathbf{r}_i]\, f_i(\theta), \quad (3)$$

where $\mathbf{k_0}$ and $\mathbf{k_s}$ are the wave vectors of the incident

and scattered electrons, respectively, and $|\mathbf{k}_0| = |\mathbf{k}_s|$ for elastic scattering.

Introducing the momentum transfer vector **s** with a magnitude of $|\mathbf{s}| = |\mathbf{k_0}-\mathbf{k_s}| = (4\pi/\lambda)\sin(\theta/2)$, and invoking the superposition principle, one obtains the amplitude of the electron wave scattered by the molecular system of N atoms as:

$$\Psi = \Sigma_{i=1,N}\Psi_i = \{\exp(ikR)/R\}\Sigma_{i=1,N} f_i(s)\exp(i\mathbf{s}\mathbf{r}_i) \quad (4)$$

The intensity of the scattered electrons can be expressed in terms of the electron current density **j:**

$$\mathbf{j(s)} = (he/4\pi m_e i)(\Psi_i^*\nabla\Psi_i - \Psi_i\nabla\Psi_i^*), \quad (5)$$

where e and m_e are the electron charge and mass, ∇ the gradient operator, and Ψ_i^* the complex conjugate wave function.

Using Eqns. (4) and (5), one obtains for the intensity:

$$\mathbf{I(s)} = I_0(\mathbf{j}_{sc}/\mathbf{j}_0) = I_0 Re\{(1/2ik_0)\Sigma_{i=1,N}(\Psi_i^*\nabla\Psi_i - \Psi_i\nabla\Psi_i^*)\} =$$
$$= (I_0/R^2)\, Re\{\Sigma_{i=1,N} f_i(s)\exp(i\mathbf{s}\mathbf{r}_i)\Sigma_{j=1,N} f_j^*(s)\exp(-i\mathbf{s}\mathbf{r}_j)\} =$$
$$= (I_0/R^2)\{\Sigma_{i=1,N}|f_i(s)|^2 + Re\,\Sigma_{i\neq j=1,N} f_i(s)f_j^*(s)\exp(i\mathbf{s}(\mathbf{r}_i-\mathbf{r}_j))\} \quad (6)$$

In equation (6), I_0 is the intensity of the incident electron beam, $\mathbf{j}_0$ ($=hk_0e/2\pi m_e$) and $\mathbf{j}_{sc}$ are the current densities for the incident and the scattered electrons, respectively. *Re* denotes the real part of the function. Higher order terms, corresponding to multiple scattering, are neglected for the current purpose.

Equation (6) is often written as $\mathbf{I(s)} = \mathbf{I}_a\mathbf{(s)} + \mathbf{I}_{mol}\mathbf{(s)}$, where the first term is ascribed the incoherent "atomic scattering" because it does not depend on the internuclear distances. The second term, which does depend on the internuclear distances, is ascribed to the coherent "molecular scattering". For each pair of atoms (i,j), separated by the instantaneous internuclear distance, $\mathbf{r}_{ij} = \mathbf{r}_i - \mathbf{r}_j$, eqn. (6) yields the molecular intensity function:

$$\mathbf{I}_{mol}\mathbf{(s)} = (I_0/R^2)\, Re\{\Sigma\Sigma_{i\neq j=1,N}|f_i(s)||f_j(s)|\exp(i\Delta\eta_{ij}(s))\times$$
$$\times\exp(i\mathbf{s}\mathbf{r}_{ij})\}, \quad (7)$$

where $\Delta\eta_{ij}(s)$ is the difference in the phase shifts incurred by the electrons while scattering from atoms i and j, respectively [31, 32].

Inherent in eqn. (7) is an approximation known as the Independent Atom Model (IAM), which assumes that the electronic wave function of each atom in a molecule is just that of the isolated atom [30]. This implies that the effects of chemical bonding on the electron density distribution of the atoms are ignored. Within the IAM approximation, the molecular surrounding of an atom does not affect its scattering, so that tabulated atomic scattering factors can be used for each atom in a molecule.

Assuming single scattering processes for fast electrons (> 10 keV) with short (attosecond) coherence time, the electrons encounter molecules that are essentially "frozen" in their rotational and vibrational states. Thus, the latter can be accounted for by using probability density functions (p.d.f.) that characterize the ensemble under investigation. If the molecular systems investigated are not at equilibrium, as is the case in studies of laser-excited molecules, a time-dependent p.d.f. must be used to describe the structural evolution of the system. In addition, rotational and vibrational motions can be separated adiabatically, since the latter involves much faster processes. The time-dependent molecular intensities can then be represented by averaging eqn. 7 with the p.d.f. that represents the spatial and vibrational distributions of the scattering ensemble [32, 33]:

$$I_{mol}(s,t) = \langle\langle\mathbf{I}_{mol}\mathbf{(s)}\rangle_{vib}\rangle_{sp} = (I_0/R^2)\times$$
$$\times\Sigma\Sigma_{i\neq j=1,N}|f_i(s)||f_j(s)|Re\{\exp[i\Delta\eta_{ij}(s)]\langle\langle\exp(i\mathbf{s}\mathbf{r}_{ij})\rangle_{vib}\rangle_{sp}\} =$$
$$= (I_0/R^2)\Sigma\Sigma_{i\neq j=1,N}|f_i(s)||f_j(s)|\cos(\Delta\eta_{ij}(s))\times$$
$$\times\int_{0,\infty} P_{vib}(r_{ij},t)[\int_{0,\pi}\int_{0,2\pi} P_{sp}(\alpha_{ij},\beta_{ij},t)\exp(i\mathbf{s}\mathbf{r}_{ij})\times$$
$$\times\sin\alpha_{ij}d\beta\alpha_{ij}]dr_{ij} \quad (8a)$$

In eqn. (8a), $\langle ... \rangle$ denotes the vibrational and spatial (orientation) averaging over the scattering ensemble, $P_{vib}(r_{ij},t)$ and $P_{sp}(\alpha_{ij},\beta_{ij},t)$ are the vibrational and spatial p.d.f., respectively, and α_{ij} and β_{ij} are the angles of the spherical polar coordinate system (Fig. 2) that define the orientation of the internuclear distance vector $\mathbf{r}_{ij}$ in the scattering coordinate frame.

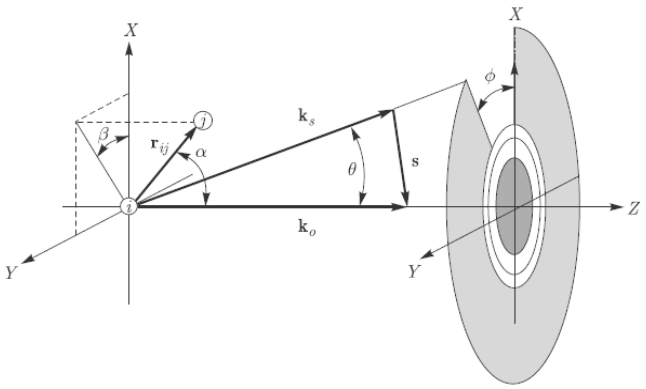

Fig. 2. Definition of scattering coordinates used for the development of intensity equations in electron diffraction. θ is the scattering angle and φ the azimuthal angle in the detector plane; k_0 and k_s are the wave vectors of the incident and scattered electrons, respectively; s is the momentum transfer vector; r_{ij} is the internuclear distance vector between the nuclei of atoms i and j, which are positioned at r_i and r_j, respectively; and α and β give the orientation of the molecular framework with respect to the XYZ laboratory frame

Рис. 2. Система координат, используемая при выводе уравнений, описывающих интенсивность рассеяния электронов. θ – угол рассеяния, φ – азимутальный угол в плоскости детектора; k_0 и k_s – волновые векторы падающего и рассеянного электронов, соответственно; s – вектор передачи импульса; rij - вектор межъядерного расстояния; α_{ij} и β_{ij} – углы в сферической системе координат, которая определяет ориентацию вектора межъядерного расстояния в координатах рассеяния

For spatially isotropic, randomly oriented molecules, $P_{sp}(\alpha_{ij},\beta_{ij}) = 1/4\pi$, and eqn. (8a) simplifies to the following expression for the time-dependent molecular intensity function:

$$I_{mol}(s,t)=(I_0/R^2)\Sigma_{i\neq j=1,N}|f_i(s)||f_j(s)|\cos(\Delta\eta_{ij}(s))\times \times\int P_{vib}(r_{ij},t)[\sin(sr_{ij})/sr_{ij}]dr_{ij} \quad (8b)$$

The time-dependent p.d.f., $P_{sp}(\alpha_{ij},\beta_{ij},t)$ and $P_{vib}(r_{ij},t)$ in eqn. (8a), determine the molecular intensity function, $I_{mol}(s,t)$ at time, t. The former describes the evolution of the spatial distribution in the system under investigation. The vibrational p.d.f. describes the evolution of structure in the ensemble of laser-excited species. In what follows, we concentrate on internuclear dynamics that evolves on a time-scale much shorter than the orientation effects, such as the rotational recurrence [10]. Therefore, only the time-independent spatial p.d.f, $P_{sp}(\alpha_{ij},\beta_{ij})$, will be considered in the current analysis. *For the particular case of a molecular ensemble at thermal equilibrium,* eqn. (8b) can be written in the form first derived by Debye [34]:

$$I_{mol}(s) \propto Re\Sigma\Sigma_{i\neq j=1,N} f_i^* f_j \langle \sin(sr_{ij})/sr_{ij}\rangle_{\mathbf{vib\text{-}rot}} = = \Sigma\Sigma_{i\neq j=1,N}|f_i||f_j|\cos[\eta_i(s)- -\eta_j(s)]\int[\sin(sr_{ij})/sr_{ij}]\,dF_T(r_{ij}), \quad (9)$$

where $F_T(r_{ij})$ is the probability *distribution* function at the vibrational temperature T, and $dF_T(r_{ij}) = P_T(r_{ij})dr_{ij}$.

As in the time-independent case, the method of averaging in eqns. (8a, b) may be defined freely, so long as certain conditions of convergence and normalization are fulfilled. The *modified molecular intensity* function sM(s,t) can be calculated as:

$$sM(s, t) = sI_{mol}(s, t)/I_{at}(s), \quad (10)$$

where $I_{at}(s)$ is the atomic background [31], considered here to be time-independent.

We now consider more generally the intensities of electrons scattered by a molecular ensemble after excitation by a short laser pulse. Let us assume that the laser field produces a *wave packet* of highly vibrationally excited states that propagates on the potential energy surface of the excited electronic state of the molecule. The time-dependent function $\Psi(r,t)$ of the wave packet can be expanded in terms of the orthonormal basis functions $\varphi_n(r)$ in the following way (see, for example, [35]):

$$\Psi(r,t) = \Sigma_{n=0,\infty} C_n\varphi_n(r)\exp(-2\pi i\, E_n\, t/h), \quad (11)$$

where n is the quantum number identifying the state with energy E_n, C_n is the amplitude, and the $\varphi_n(r)$ are a complete set of arbitrary analytic functions.

The modified molecular intensity for randomly oriented species can then be represented by [36]:

$$sM(s,t) = g(s)\int\Psi^*(r,t)\Psi(r,t)\,[\sin(sr)/r]\,dr = = g(s)\,\Sigma\Sigma_{n,m=0,\infty}\, C_m^* C_n \exp(-2\pi i\,\Delta E_{mn}t/h)\times \times\int\varphi_m^*(r)\varphi_n(r)\,[\sin(sr)/r]\,dr, \quad (12)$$

where $\Delta E_{mn} = E_m - E_n$, and g(s) is the reduced atomic scattering factors [31].

Therefore, the radial distribution function obtained from a time resolved electron diffraction (TRED) experiment, i.e., the Fourier transform F(r,t) of the modified molecular intensity sM(s,t), also depends explicitly on *both* the internuclear distances *and* the time. Thus, it contains *direct* information on the time-evolution of the molecular structure through:

$$F(r,t) = (2/\pi)^{1/2}\int sM(s,t)\exp(isr)\,ds \quad (13)$$

Applying the general form of the molecular intensities, eqn. (8b), to the one-dimensional case, it is possible to write:

$$sM(s,t) = g(s)\int P(r,t)\,[\sin(sr)/r]dr, \quad (14)$$

where $P(r,t) = \Psi^*(r,t)\Psi(r,t)$ and, consequently:

$$F(r,t) \propto P(r,t)/r \quad (15)$$

Thus, eqns. (12)-(15) show that in TRED, *the modified molecular intensities of scattered electrons depend explicitly on both the time-evolution of internuclear distances and the energy distribution*. Averaging the molecular intensity function sM(s,t) over an electron pulse profile function $I_0(t;\ t_d)$ yields the TRED diffraction intensities $sM(s;\ t_d)$, parametrically dependent on the delay time t_d between the pump laser pulse and the electron probe pulse of duration τ:

$$\langle sM(s;\ t_d)\rangle_\tau = \int_{t,t+\tau} I_0(t';\ t_d)sM(s,\ t')dt'. \quad (16)$$

In this way data refinement involves minimization of the functional:

$$\Sigma_{i=1,m}\,[\langle s_i M(\ s_i;t_d\ )\rangle_{\tau,exp} - \boldsymbol{R}\,\langle s_i M(\ s_i;t_d\ )\rangle_{\tau,theo}]^2, \quad (17)$$

where m is the number of data points and $\boldsymbol{R}$ the index of resolution.

The solution of the inverse diffraction problem is a characteristically ill-posed problem [37, 38] and is described for TRED data refinement in Chapters 2 and 4 of the monograph [11].

2. Modelling the dissociation dynamics of ICN

To illustrate the basic effects arising in the scattering time-dependent intensities and their corresponding Fourier transforms (the radial distribution functions of the inter-atomic distances), we will focus on the linear triatomic molecules (A-B-C), in which the action of a laser pulse breaks the bond A-B. In many cases, the potential function for such systems can be expressed as [39]:

$$V(R,\ r) = V_0\exp[-\ (R - \gamma r)/\rho], \quad (18)$$

where R – the distance between the nucleus A and the center of mass of the fragment B-C in the molecule A-B-C; $r = r_0(BC) - r_e(BC)$; $\gamma = m_C/(m_B + m_C)$; $r_0(BC)$ and $r_e(BC)$ – internuclear distance in the ground vibrational state and the equilibrium internuclear distance of the fragment B-C, respectively; ρ – a so-called range parameter [39, 40]. The reactions and

APES of this kind are well known for a number of the systems [39-41]. In the first stage of the analysis, it has been shown the manifestation of the nuclear dynamics in the scattering of the ultrashort pulses of the fast electrons by the systems that dissociate in accordance with the adiabatic potential functions.

The ground state of the ICN molecule is approximated by a Morse function with the parameters: a_M = 190 pm^{-1}, R_e (iodine to center-of mass distance) = 261.7 pm, D_e = 26340 cm^{-1}. The dissociative state is selected from several that are possible, and obeys Eqn. (18), with the parameters V_0 = 242720 cm^{-1}, R_0 = 262.2 pm and ρ = 80 pm, as given in refs. [41, 42].

The photodissotiation of ICN has been studied extensively both by experimental and theoretical methods, including femtosecond transient state spectroscopy (please, see ref. [43] and references therein).

The dissociation of ICN (210 < λ< 350 nm) proceeds via two channels [43, 44]:

$$ICN \rightarrow I(^2P_{3/2}) + CN(X^2\Sigma^1) \quad (19)$$

$$ICN \rightarrow I(^2P_{1/2}) + CN(X^2\Sigma^1), \quad (20)$$

producing the CN radicals predominantly in the ground electronic state $X^2\Sigma^1$, and the iodine atoms in the $^2P_{3/2}$ and $^2P_{1/2}$ states. The vibrational distribution of the CN fragment of the ICN molecule was measured [45] and at 266 nm it was found that vibrational population ratios, $n(v = 1)/n(v = 0) = 0.012$; $n(v = 2)/n(v = 0) = 6\cdot10^{-4}$; $n(v = 3)/n(v = 0) = 1\cdot10^{-4}$.

In the 266 nm photolysis, the experiment [45] determined rotational distribution of the radicals can be presented as a sum of three B_0 main distributions centered at the rotational temperatures T_1 = 37(3)K, T_2 = 489(12)K and T_3 = 6134(250)K, with approximately equal in grated fractional populations.

Rotational excitation of the CN fragments requires an additional term in the potential function, Eqn. (18), and can be approximated in diffraction intensities by including the centrifugal distortion δr of the r(CN) internuclear distance in a relatively long time range. However, considering time scale of the dissociation, the evolution of the angular momentum can be neglected.

In a series of studies (please, see, e.g., ref. [43] and references cited therein) it was shown that, at the wavelength of 306 nm, the dissociation channel leading to the iodine excited state $I(^2P_{1/2})$ is effectively closed. Thus, based on the experimental studies described in ref. [43], in our model calculations the dissociation of the ICN was assumed to proceed via a stretching reaction coordinate, and the parameters of ref. [43] for the dissociative potential leading to $I(^2P_{3/2})$ were used (please, see Eqn. 19). The molecular electron diffraction intensities, sM(s), for the molecule in their ground state were calculated with the parameters of refs. [32] and [42] using standard computational procedures [31].

One approach that can be used to describe the dynamics of the excited molecules is an approximation of the wave packet [46]. The wave packet carries the information on the relative positions and nuclear momenta, as well as their components at different APES, corresponding to different electron states [46]. For the wave function with minimal uncertainty Gaussian function can be used as the basis for the creation of the wave functions of the system, as it was proposed in the work [47-49]; please, see also [46]). Considering the classical trajectory in the phase space, where the Hamiltonian in the vicinity of the moving point $\{p(t); R(t)\}$ can be expressed in terms of the degrees of $(p - \langle p(t)\rangle)$ and $(R - \langle R(t)\rangle)$ up to the second order, the wave function is defined as follows [47]:

$$\psi(r,t) = \exp\{(2\pi i/h)[\alpha(t)(R-\langle R(t)\rangle)^2 + \langle p(t)\rangle(R-\langle R(t)\rangle) + \gamma(t)]\}, \quad (21)$$

where $\alpha(t)$ gives the spreading of the wave packet, $\gamma(t)$ – its complex phase, and $\langle ...\rangle$ – is the expected value. Using the time-dependent Schrödinger equation, we can obtain the differential equations for the position and the momentum:

$$\partial\langle R(t)\rangle/\partial t = \langle p(t)\rangle/m \text{ and } \partial\langle p(t)\rangle/\partial t = -\langle\partial V(R)/\partial R\rangle, \quad (22)$$

where $V(R)$ – the potential in the Born-Oppenheimer approximation. The equations (22) describe the trajectory of the wave packet. For large temporal delays after the excitation of the studied molecules and the use of longer probing electron pulses it should be considered the increase of the width (the spreading) of the wave packet, which manifests in the diffraction pattern. In this case, the probability density of the interatomic distances in the ensemble of the dissociated molecules can be represented as follows:

$$P(R, t) = [2\pi\sigma^2(t)]^{-1/2}\exp\{-[R - R(t)]^2/2\sigma^2(t)\}, \quad (23)$$

where $\sigma(t = 0)$ – the dispersion of the wave packet at the initial time of the laser excitation, and $R(t)$ – the classical trajectory of the center of gravity of the wave packet. Consequently, the dispersion of the propagating wave packet can be expressed as a linear function of time during its free motion:

$$\sigma(t) = \sigma(0)[1 + h^2t^2/16\pi^2m^2\sigma^4(0)]^{1/2}. \quad (24)$$

If the pulse laser pump has a form of δ-function at t = 0, the temporal dependence of the molecular intensity will be:

$$sM(s, t) = \Sigma_{i>j}g_{ij}(s)\int(\sin(sR)/R)P(R, t)dR, \quad (25)$$

where

$$P(R,t) = N\exp(-V_0\{R(t)\} - R_0)/\rho E), \quad (26)$$

$$N = \int\exp(-V_0\{R(t) - R_0\}/\rho E)dR(t) \quad (27)$$

When the form of the probing electron pulse is approximated by the Gaussian function with the

central point $t = t_0$ and corresponding duration of τ, the averaged molecular intensities can be written as:

$$\langle sM(s,t_0)\rangle_\tau = (2\pi\tau^2)^{-½} \int_{t,t+\tau} (\exp[-(t-t_0)^2/2\tau^2]\, sM(s,t)\, dt \quad (28)$$

Using the above theory, it were calculated the time-dependent intensities of the molecular scattering and the corresponding radial distributions of the internuclear distances during the processes of the photodissociation of ICN, Figs. 3 and 4 (please, see ref. [50] for comparison of the results).

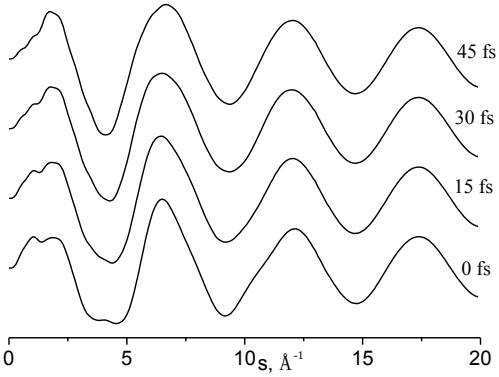

Fig. 3. Molecular intensity functions sM(s,t) calculated for the dissociation dynamics of the ICN randomly oriented molecules as a function of probe time in TRED using 300 fs electron pulses. Diffraction intensities were calculated for the photodissociation at ICN excitation from the ground state to the dissociative state (Eqn. 19)

Рис. 3. Интенсивности молекулярного рассеяния sM(s,t), рассчитанные для динамической диссоциации произвольно ориентированных молекул ICN как функции от времени регистрации TRED с использованием 300 фс электронных импульсов. Дифракционные интенсивности рассчитывались для фотодиссоциации при возбуждении молекулы ICN из основного состояния в диссоциативное (19)

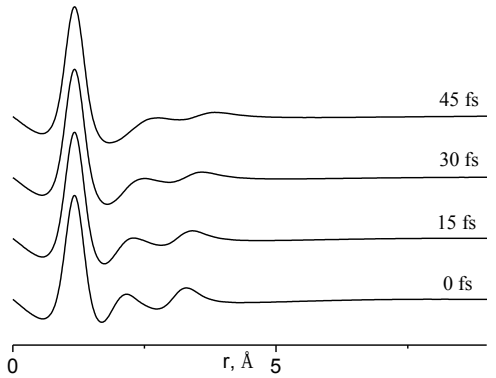

Fig. 4. Radial distribution curves F(r,t) calculated for the dissociation dynamics of the ICN randomly oriented molecules as a function of probe time in TRED using 300 fs electron pulses. Diffraction intensities were calculated for the photodissociation at ICN excitation from the ground state to the dissociative state (Eqn. 19)

Рис. 4. Функции радиального распределения F(r, t), рассчитанные для динамики диссоциации произвольно ориентированных молекул ICN как функции от времени регистрации TRED с использованием 300 фс электронных импульсов. Дифракционные интенсивности рассчитывались для фотодиссоциации при возбуждении молекулы ICN из основного состояния в диссоциативное (19)

When it is used the model of the Gaussian wave packets (eqn. (21), we can obtain the results shown in Figs. 3 and 4. From Fig. 3 it is clear that the radial distribution curves obtained with a relatively long probe pulses are significantly different from those presented in ref. [50]. However, some details of the dynamics of the wave packets still it is possible to define at a time interval, which is much shorter than the probe duration. Figs. 3 and 4 also shows that the distribution of the time-dependent wave packet can be observed using the TRED technique, if the probing electron pulse is 300 fs and can be achieved with our new TRED equipment [51].

The studies carried out in the work [50] show, that the time-dependent intensity of the electron diffraction observed for dissociative states, is strongly dependent on the shape of APES. The investigations also demonstrate that the diffraction intensities in TRED can be easily calculated for the dissociative processes, if we know the function of the potential energy. Thus, in principle it is possible to solve the inverse problem, i.e. the determination of the parameters PES using the TRED technique.

The method of reference frames and synchronization of structures

TRED method utilizes synchronized sequences of ultrafast pulses – laser pulse is utilized to initiate the reaction and electron pulses to probe the subsequent changes in the molecular structure of the sample. The time-dependent diffraction patterns are recorded using CCD-camera in the new femtosecond TRED apparatus [51]. The pulse sequence is repeated in such a way that electron pulses appear before or after the laser pulse, and in fact the images of the evolving molecular structure is performed in a continues recording mode.

One of the significant features of electron diffraction is that electron scattering occurs from all atoms and the atom-atom pairs in the molecular sample. Therefore, unlike spectroscopic techniques where a probe laser pulse is tuned to specific transitions, probing electron pulse is sensitive to all particles encountered along the way. Therefore, electron diffraction can detect structures, which are not immediately detected by spectroscopy. However, determination of the molecular structure in TRED represents a formidable challenge. Diffraction patterns represent a superposition of incoherent scattering from atoms as well as coherent molecular interference from all atom-atom pairs. Because of the lack of long-range order in gases that increase the interference of coherent interference, incoherent nuclear scattering is an order of magnitude higher that the coherent one. In addition,

due to the small fraction of molecules that undergo structural changes (typically – ~ 10% or less), a major contribution to electron diffraction pattern is made by molecules that did not undergo photoexcitation.

A key success in obtaining information about structural dynamics of a small set of molecules that undergo structural changes when the signal is much less, than the background was the application of the method of reference frames [52]. The method consists of synchronization of electron pulses in such a way that a baseline reference signal is established in situ. That is usually obtained at "negative time" (before the pump (laser)) in the ground state, or one of the evolving structures at positive times. At a different reference times (t_{ref}) it is possible to choose selected changes. Numerical methods allow for determination of the difference between each of the diffraction patterns with a time resolution and a separate reference signal. The technique is demonstrated in a number of examples (see, e.g. review article [52]).

The method of reference frames has several major advantages. First, the strong (unwanted) background signal from the atomic scattering is a common contribution to all diffraction patterns – regardless of the time delay and the nature of the reaction – and, therefore, can be virtually eliminated by calculating the difference between diffraction patterns for several time delays. Thus, despite the fact that in general, the background is dominated in the diffraction pattern, in the curve of the intensity of the reference frame molecular scattering is dominating. Secondly, any intrinsic error of the detection system will be effectively eliminated or significantly reduced by calculating the difference. Finally, each sample with selected reference frame represents the relative contribution of each reactant and the transition structures, while in the original raw data, only relatively small fraction of the signal originates from transient structures, while most of the signals are caused by unreacted components. Hence, the importance of the contribution of transitional structures increases significantly in samples with selected reference frames.

Difference method for time-dependent diffraction data analysis. The recorded diffraction patterns are dependent on the time delay between the pump (laser) and the probe (electron) pulses, $\Delta I(s; t_{ref}, t)$, are difference curves related to the structural changes of the transition state:

$$\Delta I(s; t_{ref}, t) = I(s; t_{ref}) - I(s; t). \quad (29)$$

Accordingly, for the molecular intensity functions we get (Fig. 5):

$$\Delta sM(s; t_{ref}, t) = sM(s; t_{ref}) - sM(s; t), \quad (30)$$

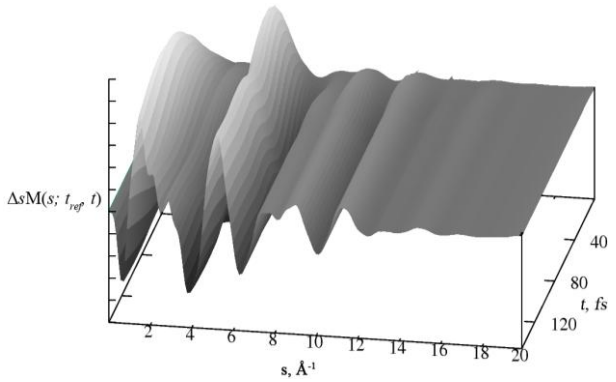

Fig. 5. Difference molecular intensity functions $\Delta sM(s; t_{ref}, t)$ calculated for the dissociation dynamics of the ICN randomly oriented molecules as a function of probe time in TRED using 300 fs electron pulses. Diffraction intensities were calculated for the photodissociation the at ICN excitation from the ground state to the dissociative state (Eqn. 19)

Рис. 5. Разностные кривые интенсивности молекулярного рассеяния $\Delta sM(s; t_{ref}, t)$, рассчитанные для динамики диссоциации произвольно ориентированных молекул ICN, как функция от времени регистрации в TRED при использовании электронных импульсов длительностью в 300 фс. Интенсивности рассеяния были рассчитаны для фотодиссоциации, когда ICN возбуждается из основного в диссоциативное состояние (19)

Accordingly, for difference radial distribution curves $\Delta F(r; t_{ref}, t)$ in the space of interatomic distances r obtained by Fourier transform of the difference curves $\Delta sM(s; t_{ref}, t)$, Fig. 6.

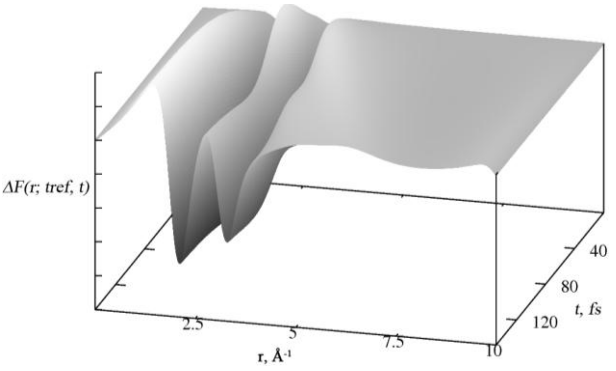

Fig. 6. Difference radial distribution curves $\Delta F(r; t_{ref}, t)$ calculated for the dissociation dynamics of the ICN randomly oriented molecules as a function of probe time in TRED using 300 fs electron pulses. Diffraction intensities were calculated for the photodissociation at ICN excitation from the ground state to the dissociative state (Eqn. 19)

Рис. 6. Разностные кривые радиального распределения $\Delta F(r; t_{ref}, t)$ рассчитанные для динамики диссоциации произвольно ориентированных молекул ICN, как функция от времени регистрации в TRED при использовании электронных импульсов длительностью в 300 фс. Интенсивности рассеяния были рассчитаны для фотодиссоциации, когда ICN возбуждается из основного в диссоциативное состояние (19)

The calculation of the theoretical equivalent of time-dependent scattering intensity with the non-equilibrium distribution in this system should be performed using a cumulant representation of the scattering intensity (please, see e.g. monograph [11], part 1 and 4]) and, for example, the stochastic approach to the analysis of the diffraction data, which has shown to be effective in TRED analysis of photodissociation of CS_2 [53]. The difference method of TRED data analysis method has demonstrated its high efficiency (please, see, e.g. review article [52]).

CONCLUSIONS

Based on model calculations presented in this article we conclude that, by TRED method, time-dependent coherent dissociation dynamics can in principle be resolved at a realistic time scale that significantly shorter than the electron pulse duration of 300 fs, which is achieved at present in a number of TRED experiments.

The study also shows that TRED intensities can be readily calculated for dissociative processes, provided the APES is known. Because of this correlation, if the TRED intensities are expressed directly in terms of the APES, solution of the inverse problem seems feasible, which provide information on coherent structural dynamics of the transient state of the chemical reaction from TRED data.

Acknowledgements

The work was supported by RFBR grant N. 16-29-11679 OFI_m and partially by RFBR grant N 14-22-02035 OFI_m.

REFERENCES
ЛИТЕРАТУРА

1. **Ischenko A.A., Golubkov V.V., Spiridonov V.P., Zgurskii A.V., Akhmanov A.S., Vabischevich M.G., Bagratashvili V.N.** A stroboscopical gas-electron diffraction method for the investigation of short-lived molecular species. *Appl. Phys. B.* 1983. V. 32. N 3. P. 161-163. DOI: 10.1007/BF00688823.
2. **Ischenko A.A., Bagratashvili V.N., Golubkov V.V., Spiridonov V.P., Zgurskii A.V., Akhmanov A.S.** Observation of the electron diffraction on the free radicals – the products of multiphoton IR dissociation of the molecules by stroboscopic gas electron diffraction. *Bull. Moscow Univ. Ser 2. Chem.* 1985. V. 26. N 2. P. 140.
3. **Ischenko A.A., Tarasov Y.I., Spiridonov V.P., Zgurskii A.V.** The study of short-lived intermediate species and structural kinetics of photoexcited molecules by stroboscopic electron diffraction. Interuniversity collection of scientific papers. The Structure and Properties of Molecules. Ivanovo: IICS. 1988. P. 63 (in Russian).
4. **Vabishchevich M.G., Ischenko A.A.** Method of studying the kinetics of fast processes. USSR Certificate number 1679907. 1991.
5. **Norrish R.G.W., Porter G.** Chemical Reactions Produced by Very High Light Intensities. *Nature.* 1949. V. 164. P. 658. DOI: 10.1038/164658a0.
6. **Tomov I.V., Chen P., Lin S.H., Rentzepis P.M.** Picosecond hard X-ray pulses and their application to time-resolved diffraction, in: Time-resolved Diffraction. Oxford: Claredon Press.1997. 456 p.
7. **Ischenko A.A., Aseyev S.A.** Time Resolved Electron Diffraction: for chemistry, biology and material science. San-Diego: Elsevier. 2014. 310 p.
8. **Minitti M.P., Budarz J.M., Kirrander A., Robinson J., Lane T.J., Ratner D., Saita K., Northey T., Stankus B., Cofer-Shabica V., Hastings J., Weber P.M.** Toward structural femtosecond chemical dynamics: imaging chemistry in space and time. *Faraday Discuss.* 2014. V. 171. P. 81-91. DOI: 10.1039/C4FD00030G.
9. **Ischenko A.A., Spiridonov V.P., Schäfer L., Ewbank J.D.** The stroboscopic gas electron diffraction method for investigation of time-resolved structural kinetics in photoexcitation processes. *J. Mol. Struct.* 1993. V. 300. P. 115-140. DOI: 10.1016/0022-2860(93)87011-W.
10. **Ewbank J.D., Schäfer L., Ischenko A.A.** Structural and vibrational kinetics of photoexcitation processes using time resolved electron diffraction. *J. Mol. Struct.* 2000. V. 524. N 1–3. P. 1-49. DOI: 10.1016/S0022-2860(99)00419-6
11. **Ischenko A.A., Girichev G.V., Tarasov Yu.I.** Electron diffraction: structure and dynamics of free molecules and condensed matter. M.: Fizmatlit. 2013. 614 p. (in Russian).
12. **Ruan C.-Y., Murooka Y., Raman R.K., Murdick R.A., Worhatch R.J., Pell A.** The Development and Applications of Ultrafast Electron Nanocrystallography. *Microsc. Microanal.* 2009. V. 15. N 4. P. 323-337. DOI: 10.1017/S1431927609090709
13. **Weber P.M., Carpenter S.D., Lucza T.** Reflectron design for femtosecond electron guns. *Proc. SPIE.* 1995. V. 2521. P. 23-30. DOI: 10.1117/12.218364.
14. **King W.E., Campbell G.H., Frank A., Reed B., Schmerge J.F., Siwick B.J., Stuart B.C., Weber P.M.** Ultrafast electron microscopy in materials science, biology, and chemistry. *J. Appl. Phys.* 2005. V. 97. N 11. P. 111101. DOI: 10.1063/1.1927699.
15. **Zewail A.H.** 4D Ultrafast electron diffraction, crystallography and microscopy. *Annu. Rev. Phys. Chem.* 2006. V. 57. N 1. P. 65-103. DOI: 10.1146/annurev.physchem.57.032905.104748.
16. **Zewail A.H.** Four-Dimensional Electron Microscopy. *Science.* 2010. V. 328. N 5975. P. 187-193. DOI: 10.1126/science. 1166135
17. **Zewail A.H., Thomas J.M.** 4D Electron Microscopy: Imaging in Space and Time. London: Imperial College Press. 2010. 360 p.
18. **Ischenko A.A.** Molecular Tomography of the Quantum State by Time-Resolved Electron Diffraction. *Phys. Res. Int.* 2013. V. 2013. P. 8.
19. **Germán S., Miller R.J.D.** Femtosecond electron diffraction: heralding the era of atomically resolved dynamics. *Rep. Prog. Phys.* 2011. V. 74. N 9. P. 096101.
20. **Ischenko A.A., Bagratashvili V.N., Avilov A.S.** Methods for studying the coherent 4D structural dynamics of free molecules and condensed state of matter. *Crystallography Reports.* 2011. V. 56. N 5. P. 751-773. DOI: 10.1134/S1063774511050129.
21. **Miller R.J.D.** Mapping Atomic Motions with Ultrabright Electrons: The Chemists' Gedanken Experiment Enters the Lab Frame. *Annu. Rev. Phys. Chem.* 2014. V. 65. N 1. P. 583-604. DOI: 10.1146/annurev-physchem-040412-110117.

22. **Miller R.J.D.** Femtosecond Crystallography with Ultrabright Electrons and X-rays: Capturing Chemistry in Action. *Science.* 2014. V. 343. N 6175. P. 1108-1116. DOI: 10.1126/science.1248488.
23. **Ischenko A.A., Aseev S.A., Bagratashvili V.N., Panchenko V.Y., Ryabov E.A.** Ultrafast electron diffraction and electron microscopy: present status and future prospects. *Physics-Uspekhi.* 2014. V. 57. N 7. P. 633-669. DOI: 10.3367/UFNe.0184.201407a.0681
24. **Campbell G.H., McKeown J.T., Santala M.K.** Time resolved electron microscopy for in situ experiments. *Appl. Phys. Rev.* 2014. V. 1. N 4. P. 041101. DOI: 10.1063/1.4900509.
25. **Kim K.T., Villeneuve D.M., Corkum P.B.** Manipulating quantum paths for novel attosecond measurement methods. *Nat Photon.* 2014. V. 8. N 3. P. 187-194. DOI: 10.1038/nphoton.2014.26.
26. **Petek H.** Single-Molecule Femtochemistry: Molecular Imaging at the Space-Time Limit. *ACS Nano.* 2014. V. 8. N 1. P. 5-13. DOI: 10.1021/nn4064538.
27. **Manz S., Casandruc A., Zhang D., Zhong Y., Loch R.A., Marx A., Hasegawa T., Liu L.C., Bayesteh S., Delsim-Hashemi H., Hoffmann M., Felber M., Hachmann M., Mayet F., Hirscht J., Keskin S., Hada M., Epp S.W., Flottmann K., Miller R.J.D.** Mapping atomic motions with ultrabright electrons: towards fundamental limits in space-time resolution. *Faraday Discuss.* 2015. V. 177. P. 467-491. DOI: 10.1039/C4FD00204K.
28. **Robinson M.S., Lane P.D., Wann D.A.** A compact electron gun for time-resolved electron diffraction. *Rev. Sci. Instrum.* 2015. V. 86. N 1. P. 013109. DOI: 10.1063/1.4905335.
29. **Plemmons D.A., Suri P.K., Flannigan D.J.** Probing Structural and Electronic Dynamics with Ultrafast Electron Microscopy. *Chem. Mater.* 2015. V. 27. N 9. P. 3178-3192. DOI: 10.1021/acs.chemmater.5b00433.
30. **Bonham R.A., Fink M.** High Energy Electron Scattering. New-York: Van Nostrand Reinhold. 1974. 318 p.
31. **Hargittai I., Hargittai M.** Stereochemical Applications of Gas-Phase Electron Diffraction. New-York: VCH Publishers, Inc. 1988. 563 p.
32. **Ischenko A.A., Schäfer L., Ewbank J.D.** Structural kinetics by time-resolved gas electron diffraction: coherent nuclear dynamics in laser excited spatially anisotropic molecular ensembles. *J. Mol. Struct.* 1996. V. 376. N 1. P. 157-171. DOI: 10.1016/0022-2860(95)09073-8.
33. **Ischenko A.A., Shafer L., Ewbank J.D.** Time-resolved electron diffraction: a method to study the structural vibrational kinetics of photoexcited molecules. New-York: Oxford University Press. 1997. P. 323-390.
34. **Debye P.** The Influence of Intramolecular Atomic Motion on Electron Diffraction Diagrams. *J. Chem. Phys.* 1941. V. 9. N 1. P. 55-60. DOI: 10.1063/1.1750826.
35. **Cohen-Tannoudji C., Diu B., Laloe F.** Quantum Mechanics. New-York: Wiley-Interscience. 1987. 887 p.
36. **Ewbank J.D., Schäfer L., Ischenko A.A.** Structural kinetics by stroboscopic gas electron diffraction 2. Time-dependent molecular intensities of predissociation processes. *J. Mol. Struct.* 1994. V. 321. N 3. P. 265-278. DOI: 10.1016/0022-2860(94)07995-1.
37. **Tikhonov A.N., Goncharsky A.V., Stepanov V.V., Yagola A.G.** Numerical Methods for the Solution of Ill-Posed Problems. M.: Nauka. 1990. 232 p. (in Russian).
38. **Tikhonov A.N., Leonov A.S., Yagola A.G.** Non-linear ill-posed problems. M.: Nauka. 1995. 312 p. (in Russian).
39. **Rapp D., Kassal T.** Theory of vibrational energy transfer between simple molecules in nonreactive collisions. *Chem. Rev.* 1969. V. 69. N 1. P. 61-102. DOI: 10.1021/cr60257a003.
40. **Levine R.D., Bernstein R.B.** Molecular Reaction Dynamics. New-York: Oxford University Press. 1974. 250 p.
41. **Herzberg G.** Electronic Spectra and Electronic Structure of Polyatomic Molecules. Florida: Krieger Pub Co. 1966. 784 p.
42. **Rosker M.J., Dantus M., Zewail A.H.** Femtosecond real-time probing of reactions. I. The technique. *J. Chem. Phys.* 1988. V. 89. N 10. P. 6113-6127. DOI: 10.1063/1.455427.
43. **Khundkar L.R., Zewail A.H.** Ultrafast Molecular Reaction Dynamics in Real-Time: Progress Over a Decade. *Annu. Rev. Phys. Chem.* 1990. V. 41. N. 1. P. 15-60. DOI: 10.1146/annurev.pc.41.100190.000311.
44. **Okabe H.** Photochemistry of Small Molecules. New-York: John Wiley & Sons Inc. 1978. 445 p.
45. **Baronavski A.P.** Laser ultraviolet photochemistry, in: Lasers as Reactants and probes in Chemistry. Washington: Howard University Press. 1985. P. 81.
46. **Garraway B.M., Suominen K.A.** Wave-packet dynamics: new physics and chemistry in femto-time. *Rep. Prog. Phys.* 1995. V. 58. N 4. P. 365.
47. **Heller E.J.** Time-dependent approach to semiclassical dynamics. *J. Chem. Phys.* 1975. V. 62. N 4. P. 1544-1555. DOI: 10.1063/1.430620.
48. **Heller E.J.** Potential Surface Properties and Dynamics from Molecular Spectra: A Time-Dependent Picture, in: Potential Energy Surfaces and Dynamics Calculations. New-York: Springer US. 1981. P. 103-131. DOI: 10.1007/978-1-4757-1735-8_4.
49. **Heller E.J.** Quantum localization and the rate of exploration of phase space. *Phys. Rev. A.* 1987. V. 35. N 3. P. 1360-1370. DOI: 10.1103/PhysRevA.35.1360.
50. **Ischenko A.A., Ewbank J.D., Schäfer L.** Structural kinetics by stroboscopic gas electron diffraction Part 1. Time-dependent molecular intensities of dissociative states. *J. Mol. Struct.* 1994. V. 320. P. 147-158. DOI: 10.1016/0022-2860(93)08011-R
51. **Mironov B.N., Kompanets V.O., Aseev S.A., Ishchenko A.A., Misochko O.V., Chekalin S.V., Ryabov E.A.** Direct observation of the generation of coherent optical phonons in thin antimony films by the femtosecond electron diffraction method. *JETP Letters.* 2016. V. 103. N 8. P. 531-534. DOI: 10.1134/S0021364016080099.
52. **Srinivasan R., Lobastov V.A., Ruan C.-Y., Zewail A.H.** Ultrafast Electron Diffraction (UED). *Helv. Chim. Acta.* 2003. V. 86. N 6. P. 1761-1799. DOI: 10.1002/hlca.200390147.
53. **Ischenko A.A., Schafer L., Luo J.Y., Ewbank J.D.** Structural and Vibrational Kinetics by Stroboscopic Gas Electron Diffraction: The 193 nm Photodissociation of CS2. *J. Phys. Chem.* 1994. V. 98. N 35. P. 8673-8678. DOI: 10.1021/j100086a015.

Поступила в редакцию 21.10.2016
Принята к опубликованию 18.11.2016

Received 21.10.2016
Accepted 18.11.2016